

## Rieske Protein from *Thermus thermophilus*: $^{15}\text{N}$ NMR Titration Study Demonstrates the Role of Iron-Ligated Histidines in the pH Dependence of the Reduction Potential

I-Jin Lin,<sup>†</sup> Ying Chen,<sup>||</sup> James A. Fee,<sup>\*,||</sup> Jikui Song,<sup>‡</sup> William M. Westler,<sup>§</sup> and John L. Markley<sup>\*,†,‡,§</sup>

Graduate Program in Biophysics, Center for Eukaryotic Structural Genomics, National Magnetic Resonance Facility at Madison, 433 Babcock Drive, University of Wisconsin, Madison, Wisconsin 53706, and Department of Molecular Biology, The Scripps Research Institute, 10550 North Torrey Pines Road, La Jolla, California 92037

Received April 19, 2006; E-mail: markley@nmrfam.wisc.edu

We have recorded  $^{15}\text{N}$  NMR spectra of oxidized, [ $^{15}\text{N}^{\delta 1}$ ,  $^{15}\text{N}^{\epsilon 2}$ ]-histidine-labeled Rieske iron–sulfur protein (Rp) from *Thermus thermophilus* (Tt) as a function of pH. Two resonances were assigned to the  $\text{N}^{\epsilon 2}$  atoms of imidazole rings bound to Fe2 of the [2Fe–2S] cluster and shown to yield  $\text{pK}_a$  values (7.46 and 9.24) that agree with those calculated from the pH dependence of the TtRp reduction potential. The data provide direct evidence for sequential dissociation of protons from  $\text{N}^{\epsilon 2}$  atoms of the two Fe-coordinated histidine rings in the oxidized protein.

As a component of the membrane-bound  $bc_1$  respiratory complex, the Rieske protein is known to play an essential role in energy transduction,<sup>1,2</sup> and the mechanism is widely thought to involve its well-studied redox behavior.<sup>2–4</sup> Rieske proteins contain a [2Fe–2S] cluster with Fe1 coordinated to two Cys  $S^\gamma$  atoms and Fe2 coordinated to two His  $\text{N}^{\delta 1}$  atoms.<sup>5,6</sup>

In the oxidized state, both metals are  $S = 5/2$  Fe(III) and coupled antiferromagnetically to yield a ground-state  $S = 0$ . Owing to the multi-state spin-ladder, Rieske protein is paramagnetic at room temperature, and this paramagnetism broadens many  $^1\text{H}$  NMR signals beyond detection. Paramagnetic relaxation depends on the square of the magnetogyric ratio  $\gamma$ . Because  $^{15}\text{N}$  and  $^{13}\text{C}$  have much smaller  $\gamma$  values than  $^1\text{H}$ , it is frequently possible to detect their NMR signals directly in paramagnetic molecules.<sup>7–9</sup> Moreover, the  $^{15}\text{N}$  chemical shifts of imidazole nitrogens can differ by 80 ppm in different protonation states,<sup>10,11</sup> making direct detection of  $^{15}\text{N}$  an attractive approach to monitor the protonation state of the histidine ligands.

All Rieske proteins have pH-dependent redox potentials,<sup>12,13</sup> and it has been proposed that protonation of the  $\text{N}^{\epsilon 2}$  atoms from the two histidine rings coordinated to Fe2 is coupled to cluster reduction.<sup>14</sup> Indeed, a detailed investigation of TtRp from pH 3 to pH 14<sup>4</sup> revealed that the pH dependence of the redox potential is determined by three  $\text{pK}_a^{\text{app}}$  values: two (7.85 and 9.65) from the oxidized state and one (12.5) from the reduced state. It is widely held that these correspond to  $\text{pK}_a$  values of Fe-bound histidine residues in the protein, and this remains the most reasonable chemical explanation of Rieske protein redox behavior, despite the lack of direct evidence. Attempts to confirm this idea involved assignment of a resonance Raman band at  $274\text{ cm}^{-1}$ , which gains intensity at high pH,<sup>15</sup> DFT/MEAD calculations,<sup>16,17</sup> interpretation of unusually short intermolecular N–N distances in crystals of TtRp,<sup>18</sup> and the observation of imidazolate signatures in the ATR-FTIR spectra of bovine Rieske protein.<sup>19</sup>

Here we incorporated [ $^{15}\text{N}^{\delta 1}$ ,  $^{15}\text{N}^{\epsilon 2}$ ]-histidine into TtRp<sup>20,21</sup> and used  $^{15}\text{N}$  NMR spectroscopy to determine the  $\text{pK}_a$  values

S<sub>38</sub>LRPREEVTPEKEPLKPGDILVYAQGGGEPKPIRLEELKPGDPFVFLAYMDDPKTKVVK  
SGEAKNTLLVARFDPPEELAPEVAQH<sub>120</sub>AAEGVVAYSAVCTH<sub>134</sub>LGCVSQF<sub>142</sub>VADEEA  
ALCPCH<sub>154</sub>GGVYDLRH<sub>162</sub>GAQVIAGPPPRVPLVPRVEDGVLVAAGEFLGPGVQA<sub>201</sub>

**Figure 1.** Sequence of the domain of *Thermus thermophilus* Rieske protein (TtRp) studied here. This protein lacks 37 N-terminal and 9 C-terminal residues of the full-length protein.<sup>18,20</sup> In addition, it contains the mutation Trp142Phe.<sup>21</sup> The four histidines of the protein are numbered, and the two histidines that ligate the iron–sulfur cluster are boxed.

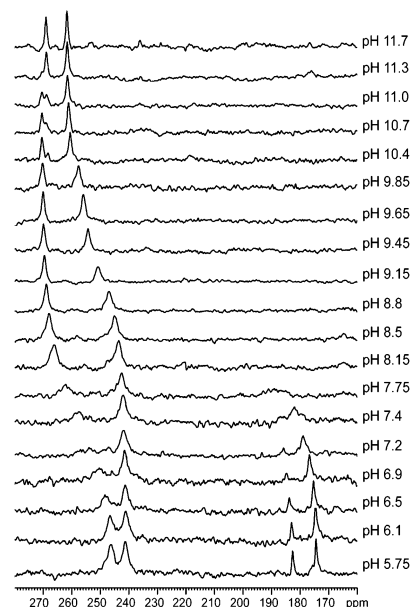


**Figure 2.** 1D  $^{15}\text{N}$  spectra of [ $^{15}\text{N}^{\delta 1}$ ,  $^{15}\text{N}^{\epsilon 2}$ ]-histidine *Thermus thermophilus* Rieske protein (TtRp) in the oxidized state at various pH values. Spectra were collected on a Bruker DMX500 NMR spectrometer with a 5 mm broadband probe at 298 K. A simple delay  $90^\circ$  acquisition pulse sequence with recycling time  $\sim 174$  ms was applied. The pH values were measured before and after data collection, and average values are reported.

of the Fe-bound histidine residues in the oxidized state of the protein.

The protein studied (Figure 1) contains four histidine residues. His120 and His162 are both on the surface of the molecule and are  $>20\text{ \AA}$  from the [2Fe–2S] cluster. His134 and His154 are bound to Fe2 of the cluster. At pH  $\sim 6$  (Figure 2), two sets of peaks were observed in the one-dimensional  $^{15}\text{N}$  spectrum. The peaks at lower frequency are sharper and insensitive to temperature (Supporting Information, S1), leading us to assign them to the imidazole  $\text{N}^{\epsilon 2}$  and  $\text{N}^{\delta 1}$  atoms of His120 and His162. This assignment was further confirmed by a heteronuclear, multiple-bond correlation experiment<sup>22</sup> that showed long-range connectivities to these peaks of the type observed only from diamagnetic residues (Supporting Information, S2).

<sup>†</sup> Graduate Program in Biophysics.

<sup>‡</sup> Center for Eukaryotic Structural Genomics.

<sup>§</sup> National Magnetic Resonance Facility at Madison.

<sup>||</sup> Department of Molecular Biology.

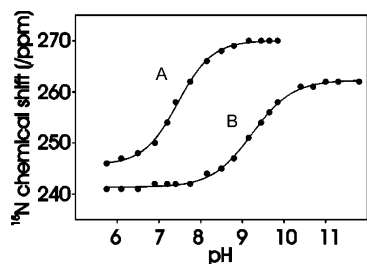


**Figure 3.** pH dependence of NMR signals (Figure 2) assigned to the  $^{15}\text{N}^{\epsilon 2}$  of each of the two histidine rings ligating Fe2 of *Thermus thermophilus* Rieske protein (TtRp). The points represent experimental data; the lines are fits to theoretical curves. (A)  $\text{p}K_{\text{a}} = 7.46 \pm 0.02$ ,  $n = 1.06 \pm 0.06$ . (B)  $\text{p}K_{\text{a}} = 9.24 \pm 0.02$ ,  $n = 0.90 \pm 0.04$ .

The broader peaks were identified with the  $^{15}\text{N}^{\epsilon 2}$  atoms of ligand histidines (H134 and H154) of TtRp. The rationale for this identification was the following: a previous study of a Rieske-type ferredoxin (T4MOC)<sup>7</sup> showed that signals from the  $^{15}\text{N}^{\delta 1}$  atoms that directly ligate iron are too broad to be detected but that broad  $^{15}\text{N}^{\epsilon 2}$  signals can be resolved; both peaks shifted upon reduction (Supporting Information, S3), as expected for histidines ligated to the iron–sulfur cluster;<sup>1</sup> the different pH dependence of the two peaks (Figure 3) indicate that they arise from different histidines.<sup>2</sup>

The pH-dependent  $^{15}\text{N}$  signals were fitted to a theoretical equation (eq 1)<sup>23</sup> in which  $\delta_{\text{obs}}$  and  $\delta_{\text{B}}$  represent the observed

$$\delta_{\text{obs}} = \delta_{\text{B}} + \frac{\Delta\delta \times 10^{n(\text{p}K_{\text{a}} - \text{pH})}}{1 + 10^{n(\text{p}K_{\text{a}} - \text{pH})}} \quad (1)$$

chemical shift of the signal at a particular pH and the chemical shift of the signal in the deprotonated state, respectively,  $\Delta\delta$  represents the titration shift of the signal from the deprotonated state to the protonated state, and  $n$  is the Hill coefficient. Fitting the titration curves yielded two distinct  $\text{p}K_{\text{a}}$  values:  $7.46 \pm 0.02$  for the peak at the higher frequency and  $9.24 \pm 0.02$  for the peak at the lower frequency (Figure 3). The signal from the histidine with  $\text{p}K_{\text{a}} = 9.24$  remained sharp throughout the transition, whereas that with  $\text{p}K_{\text{a}} = 7.46$  broadened around pH 7.5 (Figure 2) and showed the influence of a second deprotonation with  $\text{pH}_{\text{mid}} \sim 10.5$ , which may be due to Tyr158, whose phenolic OH forms a H bond to  $S^{\gamma}$  of ligand Cys132 and is only  $\sim 7 \text{ \AA}$  from Fe2.<sup>18</sup> The  $\text{p}K_{\text{a}}$  values determined here for oxidized TtRp (7.46 and 9.24) are in close agreement with those derived from the pH dependence of the reduction potential (7.85 and 9.65).<sup>4,24</sup>

Because the structures of cluster regions of the bovine Rieske protein (Irie) and TtRp (Inyk) are nominally identical, it is reasonable to make comparisons between the current results and the DFT/MEAD calculations by Ullman et al.<sup>16,17</sup> The calculations suggested that the microscopic  $\text{p}K_{\text{a}}$  of His141 of bovine Rieske protein (His134 in TtRp) is only slightly lower than the microscopic  $\text{p}K_{\text{a}}$  of His161 (His154 in TtRp): 7.1 versus 7.4. Hence, as deprotonation begins, the anionic “hole” is shared between the two imidazole rings, resulting in nonlinear Hill plots, with  $n$  deviating substantially from unity. The data of Figure 2 show clearly that the two imidazoles of TtRp undergo separate (noninteracting) deprotonation steps with  $n \approx 1$  (the NMR data fitted equally well, with  $n$  fixed at unity). The DFT/MEAD calculations for bovine Rieske protein yielded a difference of  $\sim 2$  pH units in  $\text{p}K_{\text{a}}^{\text{app}}$  and  $\text{p}K_{\text{a}}^{\text{app}}$ ; this is remarkably similar to the difference observed for TtRp (1.8). Because the lower apparent  $\text{p}K_{\text{a}}$  of the calculation was for His 141 (Tt His134), the lower  $\text{p}K_{\text{a}}^{\text{obs}}$  (7.46) of oxidized TtRp can tentatively be associated with deprotonation of His134.

Assignment of the  $^{15}\text{N}$  signal with the lower  $\text{p}K_{\text{a}}$  to His134 (lower solvent exposure than His154) is consistent with its observed

midpoint broadening and high pH perturbation by nearby Tyr158. In terms of proposed mechanisms of the  $bc_1$  complex, the consensus view is that one electron and one proton from the quinol are transferred to the Rieske protein. Subsequently, the proton from the semiquinone is believed to go to a nearby Glu residue, while the second electron is believed to go to heme  $b_L$ .<sup>1,2,4,25</sup> Assignment of the lower  $\text{p}K_{\text{a}}$  to His134 would suggest that His134 acts as the proton donor/acceptor during these oxidation/reduction steps, whereas His154 with the higher  $\text{p}K_{\text{a}}$ , which is actually located closer to the binding sites for quinol and cytochrome  $c_1$ ,<sup>1,25</sup> may remain protonated. Similar considerations are likely to apply to the closely related Rieske protein in the  $bcf$  complex.<sup>26</sup>

**Acknowledgment.** Supported by NIH grants (GM58667, J.L.M.; GM35342, J.A.F.). NMR data were collected at the National Magnetic Resonance Facility at Madison, with support from the NIH National Center for Research Resources (P41 RR02301). Labeled materials were obtained from the NIH-supported Stable Isotope Resource at Los Alamos (NIH/NIBIB 5P41 EB002166).

**Supporting Information Available:** Additional spectra used in assigning the  $^{15}\text{N}$  signals (Figures S1–S3). This material is available free of charge via the Internet at <http://pubs.acs.org>.

## References

- Zhang, Z.; Huang, L.; Shulmeister, V. M.; Chi, Y. I.; Kim, K. K.; Hung, L. W.; Crofts, A. R.; Berry, E. A.; Kim, S. H. *Nature* **1998**, *392*, 677–684 and references therein.
- Crofts, A. R.; Guergova-Kuras, M.; Huang, L.; Kuras, R.; Zhang, Z.; Berry, E. A. *Biochemistry* **1999**, *38*, 15791–15806 and references therein.
- Iwata, S.; Lee, J. W.; Okada, K.; Lee, J. K.; Iwata, M.; Rasmussen, B.; Link, T. A.; Ramaswamy, S.; Jap, B. K. *Science* **1998**, *281*, 64–71.
- Zu, Y. B.; Couture, M. M. J.; Kolling, D. R. J.; Crofts, A. R.; Eltis, L. D.; Fee, J. A.; Hirst, J. *Biochemistry* **2003**, *42*, 12400–12408.
- Gurbiel, R. J.; Doan, P. E.; Gassner, G. T.; Macke, T. J.; Case, D. A.; Ohnishi, T.; Fee, J. A.; Ballou, D. P.; Hoffman, B. M. *Biochemistry* **1996**, *35*, 7834–7845.
- Iwata, S.; Saynovits, M.; Link, T. A.; Michel, H. *Structure* **1996**, *4*, 567–579.
- Xia, B.; Pikus, J. D.; Xia, W.; McClay, K.; Steffan, R. J.; Chae, Y. K.; Westler, W. M.; Markley, J. L.; Fox, B. G. *Biochemistry* **1999**, *38*, 727–739.
- Machonkin, T. E.; Westler, W. M.; Markley, J. L. *J. Am. Chem. Soc.* **2002**, *124*, 3204–3205.
- Babini, E.; Bertini, I.; Capozzi, F.; Felli, I. C.; Lelli, M.; Luchinat, C. *J. Am. Chem. Soc.* **2004**, *126*, 10496–10497.
- Blomberg, F.; Maurer, W.; Rüterjans, H. *J. Am. Chem. Soc.* **1977**, *99*, 8149–8159.
- Drohat, A. C.; Xiao, G. Y.; Tordova, M.; Jagadeesh, J.; Pankiewicz, K. W.; Watanabe, K. A.; Gilliland, G. L.; Stivers, J. T. *Biochemistry* **1999**, *38*, 8, 11876–11886.
- Link, T. A. *Adv. Inorg. Chem.* **1999**, *47*, 83–157.
- Zu, Y. B.; Fee, J. A.; Hirst, J. *J. Am. Chem. Soc.* **2001**, *123*, 9906–9907.
- Ullmann, G. M.; Noodleman, L.; Case, D. A. *J. Biol. Inorg. Chem.* **2002**, *7*, 632–639.
- Kuila, D.; Schoonover, J. R.; Dyer, R. B.; Batie, C. J.; Ballou, D. P.; Fee, J. A.; Woodruff, W. H. *Biochim. Biophys. Acta* **1992**, *1140*, 175–183.
- Ullmann, G. M.; Noodleman, L.; Case, D. A. *J. Biol. Inorg. Chem.* **2002**, *7*, 632–639.
- Klingen, A. R.; Ullmann, G. M. *Biochemistry* **2004**, *43*, 12383–12389.
- Hunsicker-Wang, L. M.; Heine, A.; Chen, Y.; Luna, E. P.; Todaro, T.; Zhang, Y. M.; Williams, P. A.; McRee, D. E.; Hirst, J.; Stout, C. D.; Fee, J. A. *Biochemistry* **2003**, *42*, 7303–7317.
- Iwaki, M.; Yakovlev, G.; Hirst, J.; Osyczka, A.; Dutton, P. L.; Marshall, D.; Rich, P. R. *Biochemistry* **2005**, *44*, 4230–4237.
- Gatti, D. L.; Tarr, G.; Fee, J. A.; Ackerman, S. H. *J. Bioenerg. Biomembr.* **1998**, *30*, 223–233.
- The tryptophan residue at position 142 was mutated to phenylalanine using standard mutagenesis protocols. The resulting protein is spectrally and structurally identical to the wild-type, as-isolated protein (Fee, J. A. et al., to be published elsewhere).
- Bax, A.; Summers, M. F. *J. Am. Chem. Soc.* **1986**, *108*, 2093–2094.
- Markley, J. L. *Acc. Chem. Res.* **1975**, *8*, 70–80.
- The systematic difference of  $\sim 0.4$  pH between the electrochemically (recorded in 2 M NaCl) and NMR determined  $\text{p}K_{\text{a}}$  values (recorded in 0.1 M NaCl) may be due to the different ionic strengths used.
- Iwata, S.; Lee, J. W.; Okada, K.; Lee, J. K.; Iwata, M.; Rasmussen, B.; Link, T. A.; Ramaswamy, S.; Jap, B. K. *Science* **1998**, *281*, 64–71.
- Carrell, C. J.; Zhang, H.; Cramer, W. A.; Smith, J. L. *Structure* **1997**, *5*, 1613–1625.

JA0627388